CrystEngComm

ROYAL SOCIETY OF CHEMISTRY

www.rsc.org/crystengcomm

Can agitation determine the polymorphs of calcium carbonate during the decomposition of calcium bicarbonate?

Jiuxin Jiang[a,b*], Ying Zhang[a], Dongdong Xu[a], Jianing Liu[c*]

[a]School of Material Science and Engineering, Hubei University of Technology, Wuhan 430068, China

[b]Hubei Provincial Key Laboratory of Green Materials for Light Industry, Hubei University of Technology, Wuhan 430068, China

[c]Institut für Pharmazeutische Technologie, Technische Universität Braunschweig, Mendelssohnstr. 1, D-38106 Braunschweig, Germany

The influence of agitation on the polymorphs and morphologies of calcium carbonate ($CaCO_3$) during the decomposition of calcium bicarbonate ($Ca(HCO_3)_2$) solution was **semi-quantitatively** investigated in the present work. X-ray diffraction (XRD) and scanning electron microscopy (SEM) were employed to characterize the polymorphs and morphologies of $CaCO_3$ in the presence and at the absence of polyethylene glycol (PEG). At the absence of PEG, the amount of calcite increases with the strengthening of agitation, while vaterite decreases and even completely disappears. We believe that agitation contributes to the crystallization of thermodynamically stable phase and limits to crystallization of thermodynamically least stable. This belief was verified by the XRD results under the same agitation conditions in the presence of PEG. The influence of agitation on the polymorphs of $CaCO_3$ was discussed from the view of the arrangement of Ca^{2+} ions under static and stirring conditions.

Keywords: Agitation; Polymorphs; Calcium carbonate; PEG; Atom arrangement

---

* Corresponding author: Tel: +86-27-59750456, Fax: +86-27-59750454, Email address: jiuxinjiang@hotmail.com. (J. Jiang); jianing.liu@tu-braunschweig.de (J. Liu)

1. Introduction

Calcite, aragonite and vaterite are three polymorphs of $CaCO_3$. From the viewpoint of thermodynamics, calcite is the most stable phase and vaterite is the least. Calcite and aragonite are both common in biological and geological samples, but vaterite is only detected as a minor component of a few biomineralised structures, and does not exist in geological samples.[1–3] Nevertheless, vaterite has been intensively investigated due to its biological activities in the last few decades.[4–15]

Generally, the typical morphologies of calcite, aragonite and vaterite are rhombohedric/cubic, needle-like and spherical, respectively. Therefore, the crystalline structure is the determinant factor of the morphologies of single $CaCO_3$ particles. As for the factor affecting the polymorphs of $CaCO_3$, first of all, reaction system is primary. The method to prepare calcite is easy and universal due to its the highest stability, such as carbonation from $Ca(OH)_2$ slurry[16–19] or $CaCl_2$ solution,[5,20] the reaction between soluble calcium salt and carbonate,[21–22] thermal decomposition of $Ca(HCO_3)_2$,[23–24] mechano-chemical preparation from $CaCl_2$ and Na_2CO_3 powders,[25] microemulsion synthesis,[26–27] etc. However, the route to synthesis vaterite is more difficult and special.[4–15] Early study[4] proposes two typical methods for the preparation vaterite crystal, *i.e.*, aqueous and nonaqueous cabonation process. However, later research has indicated that vaterite can be obtained at room temperature when CO_2 gas is introduced into $CaCl_2$ solution in the presence of ammonia.[5–7]

Except for reaction system, some reaction parameters can also affect the polymorphs of $CaCO_3$, such as reaction temperature, reaction time, concentration of reactants, the addition of additives, etc. In fact, these parameters are usually used to control the formation of vaterite phase due to its thermodynamic instability. With the assistance of surfactants[11–13] especially block copolymers,[2,14–15] vaterite phase or its superstructures can be obtained. Reaction temperature[9,11] can also promote the formation of vaterite phase. Vaterite phase and its superstructures are easy to form inside or at the surface of ethanol/water solution.[8,12] In addition, mineralisation for a long time[2,8,13–15] is also a common method to obtain vaterite phase or its superstructures.

In fact, reaction parameters mentioned above can not only affect the polymorphs of $CaCO_3$, but also influence the morphologies of the same crystalline phase. Besides rod-like,[10–11,28–29] belt-shaped crystals,[11] spindle,[16,30] chain-like,[19] hollow sphere[31] or solid sphere[11,22] aggregated by large amount of single calcite particles under some particular conditions, the most prevailing morphology of calcite particles is rhombohedric or cubic. While except for the typical spherical morphology, single vaterite crystals are more inclined to aggregate into ellipse,[10] plate,[11] faveolate,[9] cake,[10] flower,[11–12] lens,[15] ring,[15] chain,[21] slice[9] and tube[11] under different conditions, especially the volume ratio of organic solvent to water,[12] the amount of surfactants,[11–12,15,21] temperature[9–10] and reaction time.[15]

There are many investigations on the effect of agitation on the preparation of metals,[32] alloys,[33] organic materials[34] and inorganic nonmetals.[20,35–37] All these research indicates that agitation has obvious influence on the morphologies of particles[32–33,35] especially that of aggregates.[35–36] However, the polymorphs of these materials are not affected by agitation conditions.[32,35–37] Although research on the effect of agitation on the morphologies and polymorphs of $CaCO_3$ are insufficient, similarly results are obtained.[20,38] During the carbonation of $CaCl_2$ solution, Han et al. have found that the fine vaterite particles are formed and aggregated into dense particles at low stirring rate, while the aggregated vaterite particles at high stirring rate look loosely.[20] Periago et al. have revealed that mechanical stirring can accelerate the carbonation process of $Ca(OH)_2$ slurry and slightly influence both the morphology and the particle size of $CaCO_3$ particles, but cannot change the polymorphs of $CaCO_3$.[38]

In our previous research,[23] a few leaf-like $CaCO_3$ superstructures have been observed under moderate agitation. We believe that static condition favors the formation of complex superstructures, while agitation can deform the superstructures and contribute to simple structures. In this prospective, our original purpose was to investigate the effect of the agitation on the morphology of $CaCO_3$ particles, however, the results that the agitation conditions change the polymorphs of $CaCO_3$ are far beyond our expectation.

2. Experimental section

0.6 g of $Ca(OH)_2$ (Sinopharm Ltd., Shanghai, China, >99%) was added in 1000 mL of deionized water and stirred for 30 min, followed by excessive CO_2 gas was then blown into suspension for 1 h to ensure the complete reaction between $Ca(OH)_2$ and CO_2, and the un-dissolved large $CaCO_3$ particles were filtered by filter paper to obtain saturated $Ca(HCO_3)_2$ aqueous solutions. Finally, the aqueous solution was kept in water bath at the temperature of 80 °C for 1 h under static, moderate agitation and intense agitation, and the corresponding sample number was marked as C-S, C-MA and C-IA, respectively (Note: the stirring rates of moderate and intense agitation are provided in Supplementary Information.). The final suspension was centrifuged at 8000 rpm for 10 min, the supernatant solution was discharged and sedimented particles were dried in the oven at 110 °C for 4 h. The same issue was investigated when PEG-6000 was introduced in the system. To perform it, 0.0149 g of PEG-6000 (Its weight ratio to $CaCO_3$ is about 2.0%, Sinopharm Ltd., Shanghai, China, >99%) was added in saturated $Ca(HCO_3)_2$ aqueous solution before water bath. To ensure the dissolution of PEG-6000, the system was stirred for 30 min. Then the solution was placed in water bath under the same agitation conditions as that of without PEG-6000 and the corresponding sample number was marked as CP-S, CP-MA and CP-IA, respectively.

The polymorphs of $CaCO_3$ were characterised by X-ray diffraction (XRD) (Rigaku, D/MAX-RB, Japan), **and the semi-quantitative phase compositions were calculated according to the intensities of the (110) crystallographic plane for vaterite (I_{110V}), of the (221) plane for aragonite (I_{221A}) and of the (104) plane for calcite (I_{104C}) by formula (1) and (2)[39]:**

$$X_{\mathrm{A}} = \frac{3.157 I_{221\mathrm{A}}}{I_{104C} + 3.157 I_{221\mathrm{A}} + 7.691 I_{110V}} \qquad X_{\mathrm{C}} = \frac{I_{104C} \times X_A}{3.157 I_{221\mathrm{A}}} \qquad X_{\mathrm{V}} = 1 - X_{\mathrm{A}} - X_C \tag{1}$$

$$X_A = \frac{3.157 \times I_{221A}}{I_{104c} + 3.157 \times I_{221A}} \qquad X_c = 1 - X_A \tag{2}$$

The morphologies were observed on scanning electron microscope (SEM) (JEOL JSM-6390, Japan).

3. Results and discussion

To investigate the influence of agitation on the morphologies of $CaCO_3$ particles, the particles are observed on SEM and the images under different agitation conditions are shown in Fig. 1. Rhombohedral crystals, single lamellar crystals (Fig. 1*a*), lamellar crystals and their assemblages, rod-like crystals and their assemblages (Fig. 1*b*), impeller-like assemblages from lamellar crystals (Fig. 1*c*) are found in sample C-S. Sample C-MA includes most simple rhombohedral crystals and a very small amount of simple needle-like crystals and lamellar assemblages (Fig. 1*d*). In sample C-IA, besides a very small amount of simple needle-like crystals, most particles are simple rhombohedral crystals (Fig. 1e).

Although rhombohedra or cubic, needle-like or rod-like, and spherical shapes are the typical morphologies of calcite, aragonite, and vaterite, respectively, calcite particles with the shape of belt,[11] chain,[19] rod,[10–11,28–29] spindle,[16,30] solid sphere[11,22] or hollow sphere,[31] vaterite particles of slice,[9] faveolate,[9] cake,[10] ellipse,[10] tube,[11] plate,[11] flower,[11–12] ring,[15] lens[15] or chain[21] and aragonite grains of rod or needle[40] have been obtained under different conditions. Accordingly, rhombohedral crystals are calcite, single lamellar crystals and their complexes belong to vaterite and rod or needle crystals and their assemblages are aragonite in the present work.

It is easy to understand that agitation can probably affect the morphologies of the particles especially their assemblages, however, agitation seems to obviously influence the **polymorphs** of $CaCO_3$ crystals. To further investigate the impact of agitation on the crystal type of $CaCO_3$, XRD of samples was carried out and the results are illustrated in Fig. 2. The **semi-quantitative** phase compositions calculated based on Kontoyannis and Vagenas[39] are listed in Table 1.

From Table 1 it can be found that the amount of calcite increases from about 24 to 94 wt% as the strengthening of agitation, while the amount of aragonite decreases from about 28 to 6 wt%, and vaterite decreases from 48% to 11% and even completely disappears. Therefore, we come to the conclusion that agitation contributes to the crystallization of calcite and limits to the crystallization of vaterite. **From Fig. 2*a*, the exceptionally high intense at diffraction angle of about 21 and 42.8°, it can be found the preferred orientation growth of vaterite crystals occurs on the crystallographic plane (004) and (008). The similar orientation growth has been observed by Gao et al.**[2]

To investigate the reproducibility of this work, all above samples were re-prepared under the same conditions. The XRD patterns of the corresponding samples were shown in Supplementary Information and the semi-quantitative phase compositions were also listed in Table 1, which indicates that this work has good reproducibility.

The continuous decrease in vaterite crystals as the strengthening of agitation are considered to be resulted from the least stable crystal structure of vaterite. As indicated in Fig. 3, Ca^{2+} cations and CO_3^{2-} anions arrangement layer by layer and the distances between Ca^{2+} ions in the (0001) faces of calcite and vaterite are 4.96 and 4.2 Å, respectively.[41] Therefore, calcite is thermodynamically more stable than vaterite because of the coulomb repulsion between Ca^{2+} cations. Without agitation in reaction system, the arrangement of Ca^{2+} ions is affected only by temperature, which is in favor of the crystallization of thermodynamically least stable vaterite phase.[23] **However, the formation of vaterite is probably limited by agitation because Ca^{2+} ions array in a more stable mode under disturbance.** As indicated in Fig. 4a, two Ca^{2+} ions inside the blue parallelogram move out of this crystal face. To maximally reduce the coulomb repulsion, one Ca^{2+} ion moves up (0001) face for one third of interplanar crystal spacing and the other moves down (0001) face for the same distance, as shown in Fig. 4b. The as-moved arrangement of Ca^{2+} ions is very similar with calcite, as indicated in Fig. 3a.

Our previous research has indicated that the addition of PEG-6000 promotes the crystallization of aragonite.[23] According to our suggestion above, we deduce that the amount of thermodynamically least stable vaterite will also decrease and more stable aragonite (or/and calcite) will increase as the strengthening of agitation when PEG-6000 is introduced in this reaction system due to the similar thermodynamically stability between calcite and aragonite.

To verify this deduction, 2 wt% of PEG-6000 was dissolved in $Ca(HCO_3)_2$ aqueous solution, then the system was also heated in water bath under the same temperature and agitation conditions, and the polymorphs and morphologies of the corresponding samples were characterized by XRD and SEM. Diffraction patterns and the phase composition calculated by formula (1) and (2) are illustrated in Fig. 5, and SEM images are shown in Fig. 6.

From Fig. 5 it can be found that vaterite decreases from about 16 to 12 wt% and even completely disappears as the strengthening of agitation, and the total amount of thermodynamically more stable phase, calcite and aragonite, increases from about 84% to 100%. The results well demonstrate our deduction that agitation is disadvantageous for the formation of thermodynamically least stable vaterite phase.

Rhombohedral crystals, rod-like crystals assemblages, flower-like assemblages from lamellar crystals (Fig. 6*a*), flower-like lamellar crystals assemblages with lamellar crystals on its surface (Fig. 6*b*) are found in sample CP-S. CP-MA consists of most single rod-like or needle-like crystals, a very small amount of rhombohedral crystals and leaf-like assemblages (Fig. 6*c*). While in sample CP-IA, besides a small amount of simple rhombohedral crystals, most particles are simple rod-like crystals (Fig. 6d). The SEM images are well in accordance with XRD results.

Although some complex assemblages can form when no agitation is applied in both systems, *i.e.* with and without PEG, the appearance of these assemblages, especially the assemblage of vaterite phase, is completely different, as illustrated in Fig. 1 and Fig. 6*b***.** In addition, this preparation method for $CaCO_3$ powder is a relatively new route and there is lack of understanding on the detailed reaction mechanism, nucleation, crystallization, growth of calcite, aragonite and vaterite, the effect of surfactant on the polymorphs and morphologies of $CaCO_3$, and so on. The investigation on these issues is being carried out in our group.

4. Conclusions

In summary, the effect of agitation on the polymorphs and morphologies of $CaCO_3$ during the decomposition of $Ca(HCO_3)_2$ solution in the presence and at the absence of PEG was **semi-quantitatively** investigated in the present work. Agitation can not only affect the morphologies of $CaCO_3$ particles, but also determine their polymorphs. Whether in the presence or at the absence of PEG, agitation limits the crystallization of thermodynamically least stable vaterite and favors the crystallization of stable calcite. Ca^{2+} ions are inclined to array into more stable crystal lattice under the disturbance of agitation.

Acknowledgements

This work is supported by the Open Foundation of Hubei Provincial Key Laboratory of Green Materials for Light Industry (No. 2013-2-8), Hubei Natural Science Foundation (No. 2009CDA030) and National Natural Science Foundation of China (No. 11174075, 30871996 and 31070521).

References

1. J. R. Young, S. A. Davis, P. R. Bown and S. Mann, *J. Struct. Biol.*, 1999, **126**, 195–215.

2. Y. X. Gao, S. H. Yu and X.H. Guo, *Langmuir*, 2006, **22**, 6125–6129.

3. R. Brown and K. P. Severin, *Can. J. Fish. Aquat. Sci.*, 1999, **56**, 1898–1903.

4. I. Matsushita, Y. Hamada, T. Moriga, T. Ashida and I. Nakarayashi, *J. Ceram. Soc. Jpn.*, 1996, **104 [11]**, 1081–1084.

5. G. Hadiko, Y. S. Han, M. Fuji and M. Takahashi, *Mater. Lett.*, 2005, **59**, 2519–2522.

6. Y. S. Han, G. Hadiko, M. Fuji and M. Takahashi, *J. Cryst. Growth*, 2006, **289**, 269–274.

7. A. Vecht and T. G. Ireland, *Geochim. Cosmochim. Ac.*, 2000, **64**, 2719–2725.

8. S. F. Chen, S. H. Yu, J. Jiang, F. Q. Li and Y. K. Liu, *Chem. Mater.*, 2006, **18[1]**, 115–122.

9. J. Chen and L. Xiang, *Powder Technol.*, 2009, **189**, 64–69.

10. Q. Q. Yang, Z. D. Nan, *Mater. Res. Bull.*, 2010, 45, 1777–1782.

11. Z. Y. Chen, C. F. Li, Q. Q. Yang and Z. D. Nan, *Mater. Chem. Phys.*, 2010, **123**, 534–539.

12. G. W. Yan, L. N. Wang and J. H. Huang, *Powder Technol.*, 2009, **192**, 58–64.

13. Z. X. Zhao, L. Zhang, H. X. Dai, Y. C. Du, X. Meng, R. Z. Zhang, Y. X. Liu, and J. G. Deng, *Micropor. Mesopor. Mat.*, 2011, **138**, 191–199.

14. X. H. Guo, S. H. Yu and G. B. Cai, *Angew. Chem. Int. Edit.*, 2006, **45**, 3977–3981.

15. Y. X. Gao, S. H. Yu, H. P. Cong, J. Jiang, A. W. Xu, W. F. Dong and H. Cölfen, *J. Phys. Chem. B*, 2006, **110[13]**, 6432–6436.

16. M. Ukrainczyk, J. Kontrec and D. Kralj, *J. Colloid Interf. Sci.*, 2009, **329**, 89–96.

17. J. G. Carmona, J. G. Morales and R. R. Clemente, *J. Colloid Interf. Sci.,* 2003, **261**, 434–440.

18. X. T. Shi, R. Rosa and A. Lazzeri, *Langmuir*, 2010, **26**, 8474–8482.

19. C. Y. Wang, C. Piao, X. L. Zhai, F. N. Hickman and J. Li, *Powder Technol.,* 2010, **198**, 131–134.

20. Y. S. Han, G. Hadiko, M. Fuji and M. Takahashi, *J. Eur. Ceram. Soc.* 2006, **26**, 843–847.

21. Y. X. Chen, X. B. Ji and X. B. Wang, *Mater. Lett.,* 2010, **64**, 2184–2187.

22. J. G. Yu and M. Lei, B. Cheng, *Mater. Chem. Phys.* 2004, **88**, 1–4.

23. J. X. Jiang, J. Z. Ye, G. W. Zhang, X. H. Gong, L. H. Nie and J. N. Liu, *J. Am. Ceram. Soc.*, 2012, **95 [12]**, 3735–3738.

24. D. F. Zhao, A. Buchholz, T. F. Mentel, K. P. Muller, J. Borchardt, A. K. Scharr, C. Spindler, R. Tillmann, A. Trimborn, T. Zhu and A. Wahner, *Atmos. Chem. Phys.*, 2010, **10,** 8601–8616.

25. J. Sargheini, A. Ataie, S. M. Salili and A. A. Hoseinion, *Powder Technol.*, 2012, **219**, 72–77.

26. Y. H. Shen, A. J. Xie, Z. X. Chen, W. H. Xu, H. Yao, S. K. Li, L. C. Huang, Zh. F. Wu and X. Y. Kong, *Mat. Sci. Eng. A*, 2007, **443**, 95–100.

27. L. P. Liu, D. W. Fan, H. Z. Mao, X. Fang and J. C. Hao, *J. Colloid Interf. Sci.*, 2007, **306**, 154–160.

28. Y. H. Ni, H. Y. Zhang, Y. Y. Zhou, *J. Phys. Chem. Solids*, 2009, **70**, 197–201.

29. J. X. Jiang, Y. Zhang, X. Yang, X. Y. He, X. X. Tang, J. N. Liu, *Adv. Powder Technol.*, DOI: 10.1016/j.apt.2013.10.001.

30. G. H. Wu, Y. J. Wang, S. L. Zhu and J. D. Wang, *Powder Technol.*, 2007, **172**, 82–88.

31. X. X. Ji, G. Y. Li and X. T. Huang, *Mater. Lett.*, 2008, **62**, 751–754.

32. M. Y. Guan, T. M. Shang, X. H. He, J. H. Sun, Q. F. Zhou and P. Gu, *Rare Metal Mat. Eng.*, 2011, **40(12)**, 2069–2071.

33. F. C. R. Hernández and J. H. Sokolowski, *J. Alloy. Compd.*, 2009, **480**, 416–421.

34. X. Lin, L. L. Tong, L. N. Zhao, L. L. Wang, M. Wang and W. D. Huang, *Trans. Nonferrous Met. Soc. China*, 2010, **20**, s826–s831.

35. S. Supothina and R. Rattanakam, *Mater. Chem. Phys.*, 2011, **129**, 439–445.

36. S. B. Zeng, X. L. Xu, S. K. Wang, Q. K. Gong, R. J. Liu and Y. Yu, Mater. *Chem. Phys.*, 2013, **140**, 159–167.

37. D. Zou, Y. Q. Ma, S. B. Qian, G. H. Zheng, Z. X. Dai, G. Li and M. Z. Wu, *J. Alloy. Compd.*, 2013, **574**, 142–148.

38. A. M. L. Periago, R. Pacciani, C. G. González, L. F. Vegab and C. Domingo, *J. Supercrit. Fluid.*, 2010, **52**, 298–305.

39. C. G. Kontoyannis and N. V. Vagenas, *Analyst*, 2000, **125,** 251–255.

40. Z. D. Nan, X. N. Chen, Q. Q. Yang, X. Z. Wang, Z. Y. Shi and W. G. Hou. *J. Colloid Interf. Sci.*, 2008, **325,** 331–336.

41. S. Mann, B. R. Heywood, S. Rajam and J. D. Birchall, *Proc. R. Soc. Lond. A*, 1989, **423**, 457–471.

Figure captions

Fig. 1 SEM images of $CaCO_3$ (a)–(c) 80°C, 60 mins, static; (d) 80°C, 60 mins, moderate agitation; (d) 80°C, 60 mins, intense agitation

Fig. 2 XRD patterns of $CaCO_3$ (a) 80°C, 60 mins, static; (b) 80°C, 60 mins, moderate agitation; (c) 80°C, 60 mins, intense agitation

Fig. 3 Atomic structure of (a) calcite and (b) vaterite

Fig. 4 (a) The stacking of Ca^{2+} ions in vaterite and the motion direction in the (0001) faces under agitation and (b) The stacking of Ca^{2+} ions in the (0001) faces after motion (Red ball and red parallelogram (● ▰): Ca^{2+} and corresponding crystal face moving up for one third of interplanar crystal spacing; Green ball and green parallelogram (● ▰): Ca^{2+} and corresponding crystal face moving down for one third of interplanar crystal spacing; Blue ball and blue parallelogram (● ▰): Ca^{2+} and corresponding crystal face without any motion.)

Fig. 5 XRD patterns of $CaCO_3$ (a) 80°C, 60 min, 2wt% PEG-6000, static; (b) 80°C, 60 min, 2wt% PEG-6000, moderate agitation; (c) 80°C, 60 min, 2wt% PEG-6000, intense agitation

Fig. 6 SEM images of $CaCO_3$ (a)–(b) 80°C, 60 min, 2wt% PEG-6000, static; (c) 80°C, 60 min, 2wt% PEG-6000, moderate agitation; (d) 80°C, 60 min, 2wt% PEG-6000, intense agitation

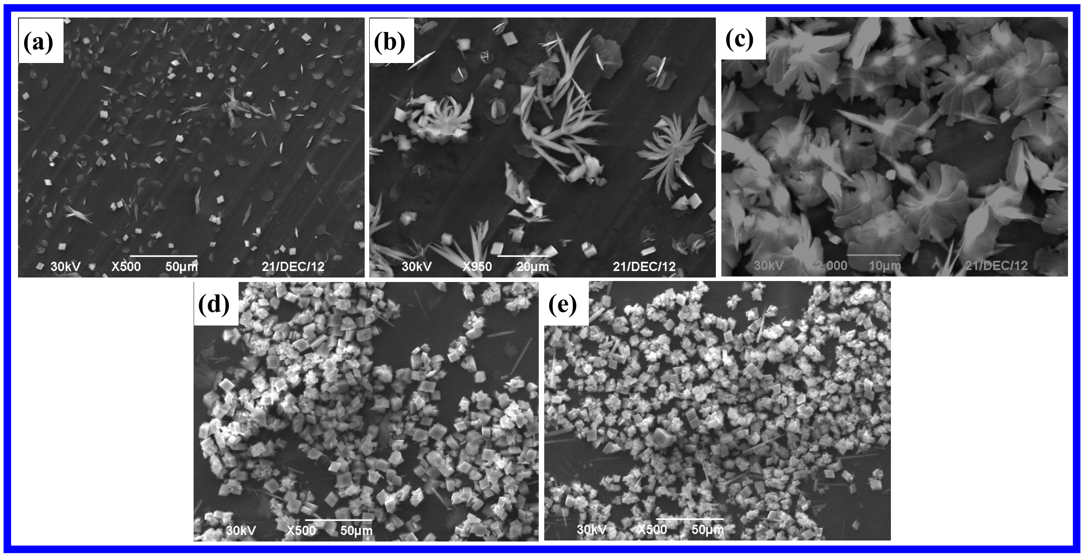

Fig. 1 SEM images of $CaCO_3$ (a)–(c) 80°C, 60 mins, static; (d) 80°C, 60 mins, moderate agitation; (d) 80°C, 60 mins, intense agitation

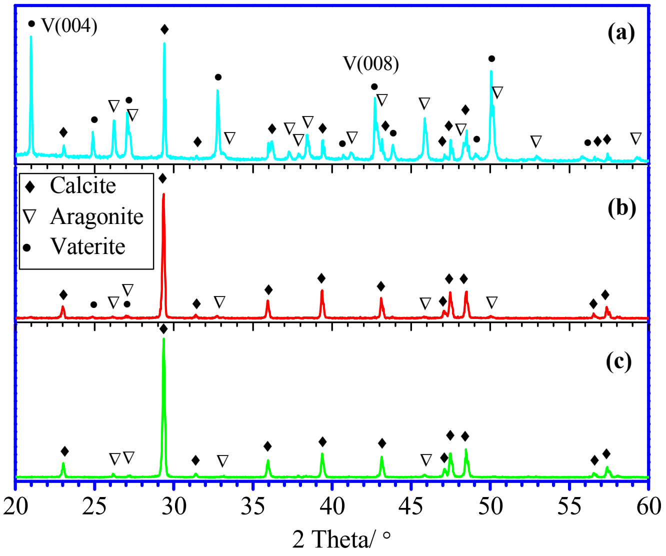

Fig. 2 XRD patterns of $CaCO_3$ (a) 80°C, 60 mins, static; (b) 80°C, 60 mins, moderate agitation; (c) 80°C, 60 mins, intense agitation

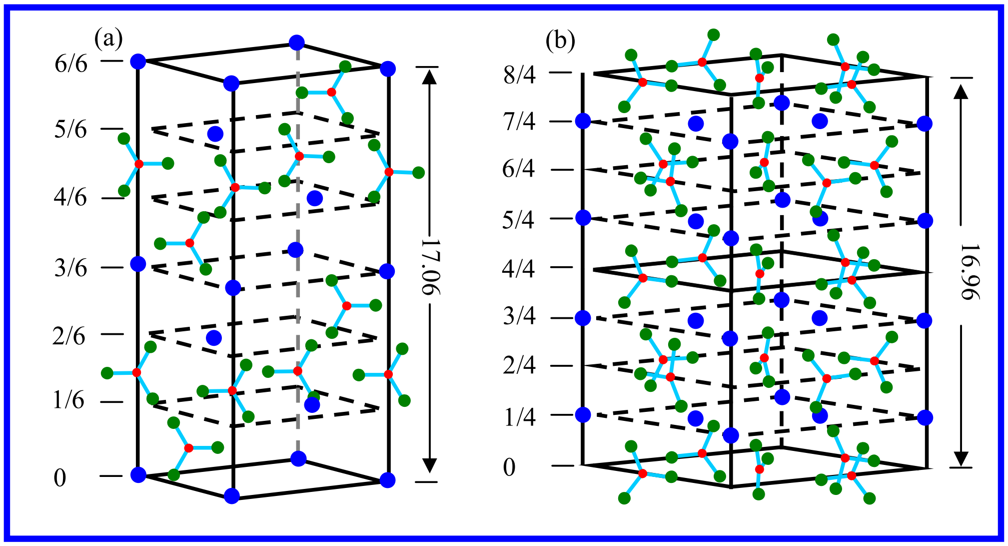

Fig. 3 Atomic structure of (a) calcite and (b) vaterite

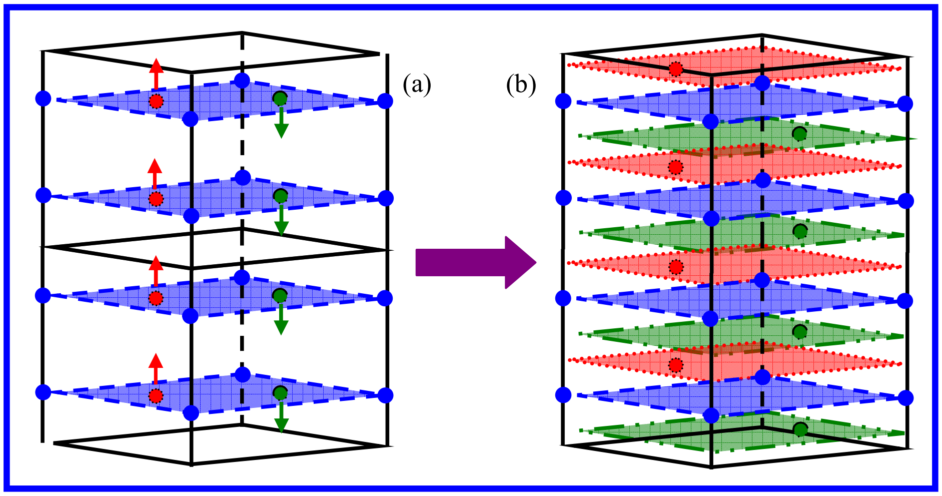

Fig. 4 (a) The stacking of Ca^{2+} ions in vaterite and the motion direction in the (0001) faces under agitation and (b) The stacking of Ca^{2+} ions in the (0001) faces after motion (Red ball and red parallelogram (● ▱): Ca^{2+} and corresponding crystal face moving up for one third of interplanar crystal spacing; Green ball and green parallelogram (● ▱): Ca^{2+} and corresponding crystal face moving down for one third of interplanar crystal spacing; Blue ball and blue parallelogram (● ▱): Ca^{2+} and corresponding crystal face without any motion.)

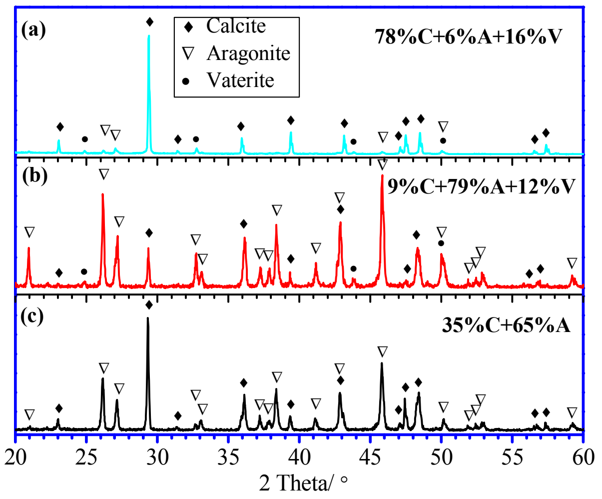

Fig. 5 XRD patterns of $CaCO_3$ (a) 80°C, 60 min, 2wt% PEG-6000, static; (b) 80°C, 60 min, 2wt% PEG-6000, moderate agitation; (c) 80°C, 60 min, 2wt% PEG-6000, intense agitation

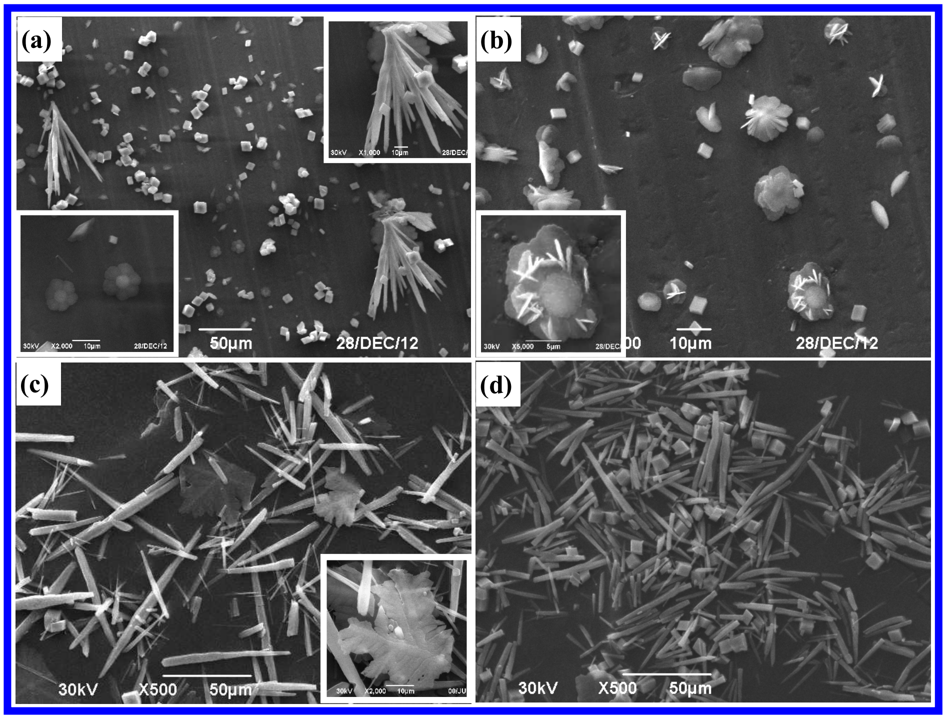

Fig. 6 SEM images of $CaCO_3$ (a)–(b) 80°C, 60 min, 2wt% PEG-6000, static; (c) 80°C, 60 min, 2wt% PEG-6000, moderate agitation; (d) 80°C, 60 min, 2wt% PEG-6000, intense agitation

Table 1 The semi-quantitative phase compositions of $CaCO_3$ prepared twice under different conditions

Reaction system and stirring rate/rpm			Phase composition			Reaction system and stirring rate/rpm			Phase composition		
			C/%	A/%	V/%				C/%	A/%	V/%
saturated $Ca(HCO_3)_2$ solution	0	1st time	24	28	48	saturated $Ca(HCO_3)_2$ solution + PEG-6000	0	1st time	78	6	16
		2nd time	24	34	42			2nd time	73	8	19
	100	1st time	85	4	11		100	1st time	9	79	12
		2nd time	84	4	12			2nd time	8	75	17
	500	1st time	94	6	0		500	1st time	35	65	0
		2nd time	93	7	0			2nd time	35	65	0

The stacking mode of Ca^{2+} ions in the (0001) faces in (a) is thermodynamically least stable due to the short distance between Ca^{2+} ions. Free of external disturbance, Ca^{2+} ions preferentially stack in this order. While agitation is exerted in reaction system, external disturbance destabilizes the stacking of Ca^{2+} ions. To maximumly reduce the coulomb repulsion, one Ca^{2+} ion moves up (0001) face for one third of interplanar crystal spacing and the other moves down (0001) face for the same distance, which corresponds to the structure of calcite.